NASA TM-87350

NASA
Technical Memorandum 87350

USAAVSCOM
Technical Report 86–C–16

Parametric Study of Beam Refraction Problems Across Laser Anemometer Windows

NASA-TM-87350

19860022385

Albert K. Owen
Propulsion Directorate
U.S. Army Aviation Research and Technology Activity—AVSCOM
Lewis Research Center
Cleveland, Ohio

June 1986

NF01536

NASA

PARAMETRIC STUDY OF BEAM REFRACTION PROBLEMS ACROSS

LASER ANEMOMETER WINDOWS*

Albert K. Owen
Propulsion Directorate
U.S. Army Aviation Research and Technology Activity - AVSCOM
Lewis Research Center
Cleveland, Ohio 44135

SUMMARY

The experimenter is often required to view flows through a window with a different index of refraction than either the medium being observed or the medium that the laser anemometer is immersed in. The refraction that occurs at the window surfaces may lead to undesirable changes in probe volume position or beam crossing angle and can lead to partial or complete beam uncrossing. This report describes the results of a parametric study of this problem using a ray tracing technique to predict these changes. The windows studied were a flat plate and a simple cylinder. For the flat-plate study (1) surface thickness, (2) beam crossing angle, (3) bisecting line - surface normal angle, and (4) incoming beam plane surface orientation were varied. For the cylindrical window additional parameters were also varied: (1) probe volume immersion, (2) probe volume off-radial position, and (3) probe volume position out of the R-θ plane of the lens. A number of empirical correlations were deduced to aid the interested reader in determining the movement, uncrossing, and change in crossing angle for a particular situation.

INTRODUCTION

The laser anemometer, in its various forms, has provided the fluid dynamicist with a powerful tool for nonintrusively measuring fluid velocities. One of the more common types of laser anemometers, the laser fringe anemometer, divides a single laser beam into two parallel beams and then focuses them to a point in space called the probe volume PV where the fluid velocity is measured.

Many of the applications using this method for measuring fluid velocities require the observation of fluids through a window. Whenever light traverses a region of a different refractive index, its direction of travel is changed in a manner described by Snell's law. The implications of this law to the laser probe volume when a window is inserted in the laser beam optical path between the focusing lens and the probe volume can be summarized as follows:

(1) The position of the actual probe volume will probably change.

---

(2) The beams will probably uncross (i.e., no longer lie in the same plane) to some extent at the probe volume location.

(3) The crossing angle of the two beams may change.

The first result means that data may not be acquired in the desired location. The second affects the data acquisition rate by distorting the probe volume, which only exists where the beams cross. The last impacts the accuracy of the measurements taken because it is directly related to the calculation of velocity by the equation

$$V = \frac{\lambda f}{2 \sin(\epsilon/2)} \tag{1}$$

where

λ laser light wavelength
f fringe crossing frequency
ϵ beam crossing angle

Most researchers have assumed that the resulting errors are small and can be ignored. There have, however, been a few attempts to assess the seriousness of this problem (refs. 1 to 3 and an unpublished alogrithm for beam crossing calculations by R.G. Seasholtz of NASA Lewis). They have, unfortunately, been concerned with special cases such as flat windows and cylinders with observations in a single plane normal to the cylinder axis of symmetry.

This report gives the results of a more general approach developed at the NASA Lewis Research Center. It uses a ray-tracing technique not restricted to special cases to study the changes in probe volume geometry and position due to refraction effects caused by both flat windows and smooth general windows. This technique follows the laser beams through any of four window shapes:

(1) Flat-plate windows (constant thickness)
(2) Cylindrical windows (constant thickness)
(3) General axisymmetric windows (constant thickness)
(4) Totally smooth general windows (variable thickness)

The technique calculates the first two cases analytically. The general axisymmetric case is treated analytically in the R-θ plane and uses a cubic spline fit in the R-Z plane. The totally smooth general window case uses the cubic spline curve fit in both the X-Y and X-Z planes. The tech nique yields the new probe volume position, the new crossing angle, and the amount of beam uncrossing specified as both the number of probe volume fringes and the absolute distance.

The technique, its use, and its capabilities will be more explicitly detailed in an upcoming NASA/U.S. Army publication of a Fortran code by the author.

Results from flat-plate and cylindrical windows are presented in this report. These two types of windows were chosen for their general applicability and because of their relative simplicity. The parameters which vary in the flat-plate case are (1) the orientation of the line connecting the lens center

and probe volume (beam bisector line) with respect to the surface normal, (2) the window thickness, and (3) the crossing angle between the two laser beams. The cylindrical window case includes these parameters as well as (4) the probe volume immersion and (5) parameters related to the nonsymmetric configurations where the beam bisector line and surface normals are not coincident.

Variations in two additional parameters have not been considered in this study. These parameters are the window or fluid indices of refraction and the laser light frequency.

SYMBOLS

$\overline{A}_1, \overline{A}_2$	incoming laser beam centerline vectors
$\|A\|$	magnitude of incoming laser beam vectors
D	total probe volume displacement
f	fringe crossing frequency
I	nondistorted probe volume immersion through cylindrical window, $(1 - R_{PV}/R_{CO})$
P	point where beam bisector crosses lens focusing plane
PV	probe volume
R_{CO}	radius of cylindrical window outer surface
R_{PV}	distance of probe volume from window axis of symmetry
T	window thickness
U	probe volume uncrossing distance
X,Y,Z	transformed coordinate system
x,y,z	primary coordinate system
X_1, Y_1, Z_1	coordinate position of intersection of lens optical plane and beam bisector
X_{PV}, Y_{PV}, Z_{PV}	original coordinate position of probe volume
Z"	line formed by intersection of lens focusing plane and plane formed by z-axis and point P
α	beam bisector angle (angle formed by intersection of beam bisector and outward surface normal where beam bisector intercepts surface)
α_1, α_2	angles formed by intersection of incoming laser beams and surface normals at point of interception

3

δ	angle, measured counterclockwise, in lens focusing plane, between Z" line and laser beams plane
ε	beam crossing angle
ε_{OR}	design beam crossing angle
θ_{PV}	angle between the X-axis and radial line passing through probe volume, measured in x-y plane
θ'_{PV}	angle between X'-axis and radial line passing through probe volume, measured in x-y plane
λ	laser light wavelength
ξ	out-of-plane angle of bisecting line relative to x-y plane, $\tan^{-1}[(Z_{PV} - Z_\ell)/(Y_{PV} - Y_\ell)]$

GEOMETRY

A basic understanding of the window and optics geometry and the variables used to describe them is necessary to correctly interpret the results given in this report. Therefore, we will take a more detailed look at the geometries of a flat-plate window and a simple cylindrical window.

Figure 1 shows the flat-plate geometry and the cylindrical window geometry. Although most of the information presented here is self-explanatory, some points should be clarified. The bisecting line is defined as a line equidistant from both laser beams and lying in the plane defined by them. It connects the lens center and the original probe volume. The beam crossing angle ε is, for all cases, the angle defined as

$$\tan \varepsilon = \frac{\left| \bar{A}_1 \times \bar{A}_2 \right|}{\bar{A}_1 \cdot \bar{A}_2} \qquad (2)$$

where

ε beam crossing angle
A incoming beam vectors

The angle α is the angle between the surface normal and the bisecting line. The original probe volume position is the probe volume position that would exist if there were no window in the optical path between the focusing lens and the probe volume. For all cases the beam plane orientation angle δ is defined as the angle, measured counterclockwise in the lens plane, made by the line connecting two beams where they cross the lens plane and a line that is either parallel to or intercepts the Z-axis and is in the lens plane. The angle ξ is the out-of-plane angle of the bisecting line relative to the x-y (R-θ) plane.

The specific restrictions to the geometries described above and in figure 1 are these:

4

(1) Surfaces must be smooth and smoothly changing.

(2) Surface slopes in the Z-direction DX/DZ must remain less than 45° for all surfaces, and DY/DZ must remain less than 45° for the general surface.

(3) The Z-axis is defined as the center of rotation for the cylindrical and general axisymmetric surface.

(4) X_1 should be greater than X_{pv}, and X_{pv} should be less than the window inner radius R_1.

RESULTS

Flat-Plate Window

The simplest window geometry used is the constant-thickness flat plate. For this case, the geometric variables are the incoming beam plane angle δ, the beam bisector off-normal angle α, the beam crossing angle ε, and the window thickness T. During this investigation, nine cases were evaluated for each of two window thicknesses and one case for a third thickness. The test cases generated are shown in table I.

A minimum beam crossing angle of 2.5° was chosen because it is near the angle used at Lewis, 9° was used for most test cases because it represents a typical crossing angle for commercial laser anemometer systems, and 18° was considered a reasonable maximum likely to be encountered. Window thicknesses of 0.3175 cm have been used at Lewis to minimize beam uncrossing problems in turbomachinery research; the 5.08-cm window thickness represents a typical wind tunnel application.

The first refraction effect to be considered is the displacement of the probe volume from the location it would occupy if a window were not located in the beam path. In general, the probe volume will be displaced in all three coordinate directions. However, for values of α near 0°, the principal displacement direction is the x direction. Although the ray-tracing technique used calculates all three components of the probe volume displacement, only the total displacement, defined as the vector sum of the x, y, and z displacements, are presented here.

Figure 2 shows the relative total probe volume displacement (total probe volume displacement/window thickness) versus the beam plane orientation angle δ for four beam bisector off-normal angles α. The total beam displacement is a linear function of window thickness; dividing by the window normal thickness therefore removes the window thickness as a variable. Furthermore, the results not shown here indicate that displacement is only a weak function of beam crossing angle in the range considered (2.5° to 18°). The difference between the extremes is normally less than 0.5 percent.

We can conclude that for a flat plate (1) the effects of crossing angle on a probe volume displacement are negligible and (2) the curves tend to collapse to the same curve when displacement is divided by window thickness, giving results that are functions only of α and δ.

Notice also that, as α changes from vertical to 55°, the ratio of probe volume displacement D to window thickness T increases. That ratio D/T increases from 0.343 to 0.555 for δ = 0° and from 0.343 to 0.862 for δ = 90°.

Figure 3 shows the relative displacement as a function of the bisector line off-normal angle for four values of δ. It is obvious that, for the range of interest, the relative probe volume displacement is a smoothly varying function dependent only on the two variables α and δ (0° $\leq \delta \leq$ 90°). There are a number of ways this relation can be empirically modeled. The equation

$$\frac{D}{T} = \left(\frac{\alpha}{55}\right)^2 (A\alpha + B) + (C\alpha^3 + K\alpha^2 + E\alpha) + (F + G\delta)\delta^2 + H \qquad (3)$$

where

A	0.0011317	E	0.0002498
B	0.1459327	F	0.0003703
C	-4.912381×10^{-7}	G	-2.7×10^{-6}
K	0.000134765	H	0.34307

closely follows the results over the given range with all errors being less than 5 percent. Here, since the curve is symmetrical about the δ = 90° line, the relation is only fitted for δ from 0° to 90°.

Beam uncrossing occurs when the two laser beams forming the probe volume no longer lie in the same plane. This phenomenon results when the two beams have different angles with respect to the surface normal as they enter the window (fig. 1). This situation occurs whenever α is nonzero while δ is not zero or 90°.

Remember that when a light beam crosses a surface into a region of different refractive index, its direction is changed in accordance with Snell's law. Snell's law requires that the new beam vector remain in a plane described by the incoming beam and the surface normal at the point of beam entry.

Figure 4 shows the uncrossing expressed as the number of fringes that can occur as a function of δ. This figure is for a beam wavelength of 5145 A, an α of 40°, an ϵ of 9°, and two window thicknesses, 1.27 and 0.3175 cm. Note that even for a thin window, over 15 fringes can be lost at certain beam plane orientations. The thicker window leads to even more severe uncrossing problems, with 30 or more fringes lost over two-thirds of the possible beam orientation range. One popular commercial system with a comparable crossing angle (9.82°) has only 28 fringes in its probe volume when the focusing lens is 480 mm.

Figure 5 shows the amount of relative beam uncrossing versus δ. The first curve is for three values of crossing angle (ϵ = 2.5°, 9°, and 18°). The second curve is plotted for ϵ of 9°, but the curves for all are similar and all collapse to nearly the same curve when divided by sin ϵ. Variations in uncrossing between crossing angles over the range of interest (2.5° to 18°) for this nondimensionalized curve are less than 2 percent. This curve can be represented by the equation

$$\frac{U}{T \sin \varepsilon} = A \sin \delta \cos \delta \qquad (4)$$

where

U   probe volume uncrossing distance
T   window thickness
A   0.42103855

Figure 5 also shows that the beam uncrossing drops to zero when $\delta = 0°$ and $\delta = 90°$. In the former case, the two beams form included angles with respect to the surface normals that are the same magnitude, and the orientation of the planes formed with the beam surface normal are mirror images. This results in equal displacement of the beams in the direction of the surface normal and equal but opposite displacement with respect to each other. Thus, although the probe volume is displaced, no uncrossing occurs.

Uncrossing also disappears at $\delta = 90°$. Here the two laser beams and the surface normals all lie in the same plane. Since Snell's law constrains the beams to remain in the original plane during refraction, the beams must continue to cross. For the same reason, if the beam bisector off-normal angle is zero, uncrossing cannot occur regardless of the value of δ.

Figure 6 is a plot of uncrossing versus bisector off-normal angle for $\delta = 40°$. This curve can be approximated by the equation

$$\frac{U}{T} = A \sin^3\alpha + B \sin^2\alpha + C \sin \alpha \qquad (5)$$

where

A   0.0741012354
B   -0.025486926
C   0.0107473369

This equation follows the plotted curve within 0.1 percent over the range of interest (0° to 55°).

From equations (4) and (5) and the the crossing angle relation, it is possible to describe the uncrossing that occurs when a laser anemometer is used to observe the flow on the far side of a flat-plate window of constant thickness:

$$\frac{U}{T} \sin \varepsilon = (A \sin^3\alpha + B \sin^2\alpha + C \sin \alpha)\sin \delta \cos \delta \qquad (6)$$

where

A   0.9619922361
B   -0.3308747123
C   0.1395233773

Errors are less than 3 percent over the range of interest, $\varepsilon = 2.5°$ to 18° and α up to 55°.

Before moving on to the case of the simple cylinder, we should mention the additional potential problem of a change in the crossing angle of the two beams as they pass through a window. This very real problem will not occur in the flat-plate case. It results from a change in the surface normal orientations between the locations where the two crossing beams enter and exit the window region. Since the surface normal orientation is constant for the flat plate, this problem will not occur.

Cylindrical Window

The addition of curvature effects that result from the use of a simple cylindrical window substantially increases the complexity of the problem. Fortunately, the window surfaces can still be described analytically.

The three new variables that are added as a result of the window curvature are

(1) Probe volume immersion (i.e., the distance between the probe volume and window)

(2) Probe volume or lens movement in the direction of curvature (the $R-\theta$ plane)

(3) Probe volume or lens movement perpendicular to the direction of curvature (the $R-Z$ plane)

The cases selected for the cylindrical window are listed in table II. They include several window thicknesses, crossing angles, immersions, four series of off-radial positions in the direction of curvature, and one series of off-radial positions perpendicular to the plane of curvature.

Figure 7 shows the relative total probe volume displacement D/T versus beam plane orientation. It is plotted for three values of immersion (0.2, 0.5, and 0.9) and an window outer radius of 25.4 cm. An immersion of zero corresponds to the probe volume being located on the window outer surface; an immersion of 1.0 corresponds to the probe volume being located on the cylindrical window centerline ($R = 0$).

At all immersions the laser anemometer sees a "flat plate" window when δ is zero. Then as δ increases toward 90°, the laser beams encounter increasingly severe curvatures. This means that the angle between the surface normals and the incoming laser beam is reduced, leading to smaller probe volume displacements. Figure 8 presents this information in a slightly different way. Here the relative total probe volume displacement is plotted versus immersion for three values of δ. Note that as the immersion increases for $\delta = 90°$ the amount of movement decreases. In the limit of $I = 1$, no displacement would occur since the surface normals for both beams would be coincident with the incoming laser light.

Although the effects of window thickness on probe volume displacement for a flat-plate window are nearly linear, this is not the case for more complex curved surfaces. In figure 9, the change in relative total probe volume displacement versus window thickness is plotted for two probe volume immersions.

8

Displacement increases by almost 30 percent at an immersion of 0.2 and over 16 percent at an immersion of 0.9. This is for an increase of 16 times in window thickness (from 0.3175 to 5.08 cm).

The change in absolute movement, however, remains relatively small. For I = 0.2, the error change in position caused by using the smaller thickness number is 1.8 mm. If this size error is acceptable, it becomes reasonable to consider approximating the probe volume relative displacement with a relation which is a function only of I and δ. If this is done, the relative total probe volume movement can be approximated as

$$\frac{D}{T} = A - B(1 - \cos 2\delta) \, (CI^3 + GI^2 + EI + F) \qquad (7)$$

where

A	0.34309	G	−0.550042
B	0.171545	E	1.787109
C	−0.229008	F	−0.00080582

Figure 10 is a plot of uncrossing versus δ at several immersions. It is plotted in fringes for a light wavelength of 5145 A. The increased uncrossing with increased immersion is simply the result of greater curvature effects. For small immersions, the window looks more like a flat plate, where no uncrossing would occur for this probe volume and lens configuration. Still, for a thicker window, the uncrossing remains over 30 fringes for a substantial portion of the range even at the shallower immersions. Considering the fact that many probe volumes contain fewer than 30 fringes, the uncrossing could destroy the probe volume entirely for many geometries.

Figure 11 shows the relative beam uncrossing nondimensionalized with respect to the window thickness for two immersions. In contrast to the flat-plate case, the effects of window thickness are not removed entirely by normal-izing the uncrossing with respect to the window thickness, particularly at smaller immersions. However, the effects are small. An increase of window thickness by a factor of 4, from 0.3175 to 1.27 cm, gives a difference between nondimensional uncrossing values of up to 16 percent.

It is apparent from figures 10 and 11 that the curves are similar and can be modeled empirically. The effects of δ are modeled within 1 percent with the equation

$$\frac{U}{T} = A \sin \delta \cos \delta \qquad (8)$$

where A = 0.533472648.

Figure 12 shows the effects of crossing angle ε on the relative beam uncrossing. In the cylindrical window case the effects of crossing angle can, as in the flat-plate case, be nearly eliminated by multiplying by the sine of the crossing angle. For example, at an immersion of 0.2, the difference between the value of uncrossing at 9° and uncrossing at 2.5° multiplied by the ratio of sin(9°) divided by sin(2.5°) is just over 1 percent at δ = 40°. Figure 12 also shows the effects of immersion on the beam uncrossing.

9

Figure 13 shows the change in relative beam uncrossing versus probe volume immersion for three crossing angles and δ = 40°. For a cylindrical window, the beam crossing angle can have a noticeable effect on uncrossing. This is due to the relation of the window arc subtended to the crossing angle. The larger the crossing angle, the greater the possible difference between the incoming beam orientation and the respective surface normal. Note that uncrossing increases as immersion increases.

Nonetheless, the similarity of the curves would indicate that the effects of immersion can be modeled empirically. An empirical relation that models immersion effects within 1 percent over the range of interest is

$$\frac{U}{T} = AI^3 + BI^2 + CI \qquad (9)$$

where

A   -0.0023071429
B   -0.0231383333
C   0.0518599524

Combining all these effects gives the following empirical equation

$$\frac{U}{T \sin \epsilon} = (AI^3 + BI^2 + CI)(1 + DT) \sin \delta \cos \delta \qquad (10)$$

where

A   0.361688894
B   -0.142271458
C   -0.515813444
D   0.15809583

This equation is accurate within 16 percent over the following ranges: $0.2 \leq I \leq 0.9$, $0 \leq \delta \leq 90$, $2.5 \leq \epsilon \leq 9$, and $0.3175 < T < 1.27$ cm. The greatest errors occur with $\epsilon = 9°$, $I = 0.2$, and $T = 1.27$ cm. Here, of course, the combination of greater crossing angles and shallow immersions results in the most severe conditions.

The last question to be addressed in this geometric configuration is the effects of cylindrical windows on beam crossing angle. Unlike the flat-plate case, the surface normals change orientation with respect to position on the surface. This means that a light beam exiting a cylindrical window may not have the same orientation that it entered with. This implies a different crossing angle. Figure 14 shows the change in crossing angle versus δ for two window thicknesses and two immersions. Notice that for the thinner window (T = 0.3175 cm), the change does not exceed 0.4 percent. The worst cases being with small immersions, thicker windows, and large values of δ.

The effects of immersion appear nearly linear at a given δ and thickness, so this effect can be modeled by an analytical relation, if a point on the curve is known. In fact the change in crossing angle can be modeled by using the relation

$$\frac{\varepsilon - \varepsilon_{OR}}{\varepsilon_{OR}} = AI \sin \delta \qquad (11)$$

where A = 0.08563. Errors for this equation are normally less than 5 percent.

All the optical configurations considered for the cylindrical window up to this point have been symmetrical in that the surface normal has been coincident with the beam bisector at the points where the beam bisector intersects the window surfaces. Let us now explore what happens when this is not true. Consider figure 15(a). Here we have introduced an asymmetry in one direction by moving the probe volume and lens center in the R-θ plane in such a manner that the beam bisector remains parallel to the x-axis. This movement, at a constant probe volume radius can, by the appropriate x-y coordinate rotation, be made to describe all geometries where the beam bisector remains in the R-θ plane (fig. 15(b)). In other words, a case in which the beam bisector forms an angle θ_{PV} with respect to the x-axis is equivalent to a case in which the beam bisector is parallel to the x'-axis and the probe volume location is specified by R_{PV} and θ_{PV}.

Figure 16 shows the relative total probe volume displacement for three θ_{PV} angles. Here the immersion is 0.1; crossing angle, 9°; thickness, 1.27 cm, and cylinder outer radius, 25.4 cm. The plots remain symmetrical with respect to δ, but the nonaxisymmetric geometry results in variations in the shape of the curve. Note that the probe volume displacement is most nearly constant for θ_{PV} = 45° and that over much of the plot it is greater than that for θ_{PV} = 60°. Remember this plot does not give any indication of the position of the probe volume, which does change as δ changes. It merely indicates that the total change at θ_{PV} = 45° is nearly constant.

Figure 17 gives the probe volume displacement versus θ_{PV} for three δ and the same geometry as figure 16. Note that for θ_{PV} between 0° and 45°, δ has little effect on the total probe volume movement, with an increase of less than 20 percent at δ = 0°. However, as θ_{PV} increases beyond 45°, the effects of a change in δ become very prominent.

Figure 18 provides the relative beam uncrossing versus for three θ_{PV} (0°, 45°, and 60°). The curves are for an immersion of 0.1, a crossing angle of 9°, and a window thickness of 1.27 cm. Note that for these conditions the situation improves as θ_{PV} increases up to about 45° and then deteriorates.

Figure 19 displays the uncrossing in number of fringes versus θ_{PV} at δ = 40°. There are two immersions and two window thicknesses plotted. The problem becomes more severe as immersion decreases and window thickness increases. For the shallow immersions it may be possible to reduce the severity of the uncrossing by selecting a nonsymmetric configuration. In any event, a surface normal – beam bisector angle of greater than 45° (θ_{PV} = 50°, in this case) is probably never warrented.

Figure 20 shows the effects of θ_{PV} on the change in crossing angle at δ = 90° and at two immersions and two thicknesses. The change in crossing angle is more severe for thicker windows and shallower immersions and goes to zero at δ = 90°. This interesting fact, explained in detail by Bicen (ref. 2), is caused by the two beams becoming, in essence, the same geometrically. Then the amount of change in the beam direction through the window is the same for

both, and the crossing angle remains the same. This figure would indicate that the change in crossing angle would be less than 3 percent over the most reasonable θ_{PV} and window thickness selections.

The last variation in geometry that we will consider occurs when the bisector line does not remain in the R-θ plane. Consider the sketch in figure 21. For the purposes of this study, the lens center was moved out of the R-θ plane in such a manner as to keep the Y position of the lens equal to the Y position of the probe volume. Then the Z position was adjusted so that ξ remained constant where

$$\tan \xi = \frac{Z_{PV} - Z_\ell}{Y_{PV} - Y_\ell} \tag{12}$$

where

ξ angle defining out-of-symmetry in Z-direction
Z position of probe volume Z_{PV} or lens Z_ℓ in axial direction
Y position of probe volume Y_{PV} or lens Y_ℓ in Y-direction

The value of ξ selected was 20°. The other geometric variables remained the same as in the previous case with the cylinder outer radius equal to 25.4 cm, the window thickness, 0.3175 cm; the immersion, 0.1; and the crossing angle, 9°.

Comparing figures 15 and 21 shows an increase in relative total probe volume displacement. At $\theta_{PV} = 0°$, the total movement increase is over 20 percent; at $\theta_{PV} = 60°$, the increase is over 10 percent. Note the flattening at the bottom of the curve ($\delta \sim 80°$) when $\theta_{PV} = 60°$. At shallower immersions or thicker windows, a double minimum can occur.

Figures 22 shows the beam uncrossing in number fringes and the relative beam uncrossing for a thin window (T = 0.3175 cm), a crossing angle of 9°, a light wavelength of 5145 A, immersion of 0.1, and a δ of 20°. Three curves are plotted ($\theta_{PV} = 0°$, 30°, 60°). The amount of uncrossing is "small" at 10 fringes or less up to approximately 30°. Even for $\theta_{PV} = 60°$, the uncrossing remains less than 25 fringes.

The final figure (fig. 23) shows the change in crossing angle for the same geometry as figure 22. Once again, conditions are much less severe for smaller θ_{PV}, with the change in crossing angle less than 0.7 percent for $\theta_{PV} \le 30°$.

CONCLUSIONS

We can draw the following conclusions for the flat-plate window:

1. Errors in probe position, crossing angle, and uncrossing can be substantial for thicker windows and large off-normal beam bisector angles. The displacement is as much as 0.343 T for $\alpha = 0°$ and twice that for $\alpha = 55°$.

2. The relationship between the beam orientation angle and refraction effects must be considered. It is possible to change the actual probe volume position noticably when measuring different velocity components by changing the value of δ.

3. The magnitude of the total probe volume displacement can be approximated to within 1 percent by

$$\frac{D}{T} = \left(\frac{\alpha}{55}\right)^2 (A\alpha + B) + (C\alpha^3 + K\alpha^2 + E\alpha)(F + G\delta)\delta^2 + H \qquad (3)$$

where α is beam bisector angle, D is probe volume displacement, T is thickness, δ is beam plane orientation angle ($0° \leq \delta \leq 90°$), and

A 0.0011317   F 3.703×10^{-4}
B 0.1459327   G -2.7×10^{-6}
C -4.912381×10^{-7} H 0.34307
K 1.34765×10^{-4} E 2.498×10^{-4}

4. The problem of beam uncrossing can be substantial even for relatively thin windows (0.3175 cm) if the angle α between the surface normal and the beam bisector is larger than 30°. The beam crossing angle has relatively minor effects on the beam uncrossing.

5. The magnitude of uncrossing can be accurately approximated by using the relation

$$\frac{U}{T \sin \epsilon} = (A \sin^3\alpha + B \sin^2\alpha + C \sin \alpha)\sin \delta \cos \delta \qquad (6)$$

where U is probe volume uncrossing distance, ϵ is beam crossing angle, and

A 0.9619922361
B -0.3308747123
C 0.1395233773

We can draw the following conclusions for the cylindrical window:

1. The addition of curvatures in one direction of a window substantially increases the complexity of the uncrossing and probe volume displacement phenomena and can result in the modification of the beam crossing angle.

2. Window curvature can effect the displacement of a probe volume to the point where, for special cases, the displacement becomes zero. This implies that it may be possible, in specific cases, to design a window where no modification of the probe volume geometry need occur.

3. For the case where the beam bisector is coincident with a window surface normal, the total relative displacement can be approximated within 16 percent by using the empirical relation

$$\frac{D}{T} = A - B (1 - \cos 2\delta)(CI^3 + GI^2 + EI + F) \qquad (7)$$

where

A 0.34309   G -0.550042
B 0.171545   G 1.787109
C -0.229008 F -0.00080582

13

4. For the case where the beam bisector is coincident with the window surface normal, the relative beam uncrossing can be approximated to within 10 percent by using the equation

$$\frac{U}{T \sin \varepsilon} = (AI^3 + BI^2 + CI)(1 + DT) \sin \delta \cos \delta \tag{10}$$

where I is immersion and

A   -0.36168894
B   -0.142271458
C   -0.515813444
D   0.15609583

5. For the case when the beam bisector is coincident with the surface normal, the change in crossing angle versus immersion for a given δ, thickness, and cylinder radius appears nearly linear and the change in crossing angle can be modeled by

$$\frac{\varepsilon - \varepsilon_{OR}}{\varepsilon_{OR}} = A(I \sin \delta) \tag{11}$$

where A = 0.08563.

6. Moving the geometry into a nonsymmetric configuration greatly increases the probe volume displacement. Displacement can be increased by 20 percent at $\theta_{pv} = 0°$ and by 10 percent at $\theta_{pv} = 60°$, with $\xi = 20°$.

7. Beam uncrossing can be a serious problem even for relatively thin windows (0.3175 cm).

REFERENCES

1. Boadway, J.D.; and Karahan, E.: Correction of Laser Doppler Anemometer Readings for Refraction at Cylindrical Surfaces. DISA Information, no. 26, Feb. 1981, pp. 4-6,31.

2. Bicen, A.F.: Refraction Correction for LDA Measurements in Flows with Curved Optical Boundaries. TSI Quarterly, vol. 8, no. 2, Apr.-June 1982, pp. 10-12.

3. Edwards, R.V.; and Bybbs, A.: Refractive Index Matching for Velocity Measurements in Complex Geometries. TSI Quarterly, vol. 10, no. 4, Oct.-Dec. 1984, pp. 3-11.

TABLE I. – GEOMETRIES EXAMINED
FOR FLAT-PLATE WINDOW CASE

Crossing angle, ε deg	Thickness T, cm	Off-normal angle, α, deg
2.5	0.3175	0,40,55
	5.08	0,40,55
9.0	0.3175	0,20,40, 45,55
	1.27	40
	5.08	0,20,40,55
18.0	0.3175	0,55
	5.08	0,55

TABLE II. – GEOMETRIES EXAMINED FOR CYLINDRICAL WINDOW CASE

Crossing angle, ε, deg	Probe volume angle, θ_PV, deg	Out-of-plane angle, ξ, deg	Cylinder outer radius, R_{CO}, cm	Thickness, T, cm	Immersion, I, percent
2.5	0	0	25.4	0.3175	0.2,0.9
5.0				.3175	0.2,0.5,0.8,0.9
9.0				.3175	0.1,0.2,0.3, 0.5,0.8,0.9
				1.27	0.1,0.2,0.3,0.9
				2.54	0.2
				5.08	0.2,0.4,0.6,0.8
	30,45,60,85			.3175	0.1
	15,45,60, 75,85			.3175	0.3
	15,30,45, 60,75			1.27	0.1
	0,30,45,60			1.27	0.3
	0,30,45,60	20		.3175	0.1
	0	0	12.7	.3175	0.2,0.8
			12.7	5.08	0.6
			25.4	2.54	0.2
			50.8	5.08	0.2,0.4,0.6,0.8
			50.8	.3175	0.2,0.4,0.8
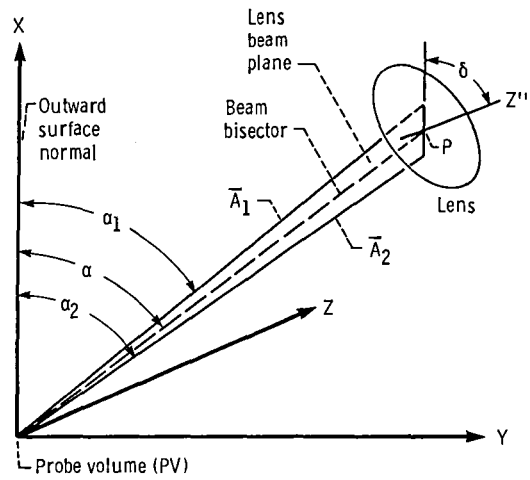
(a) Flat plate.
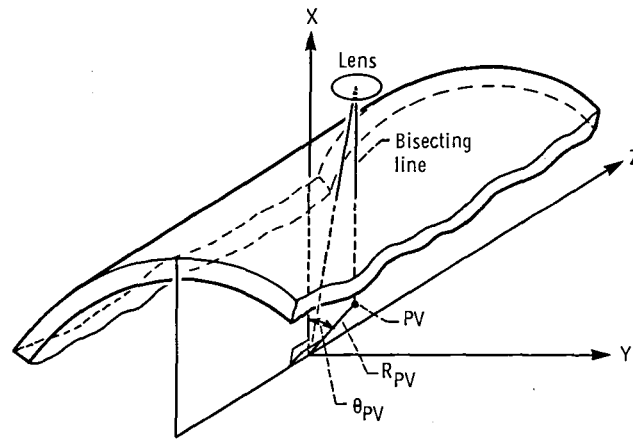
(b) Simple cylinder.

Figure 1. – Window geometry and nomenclature.
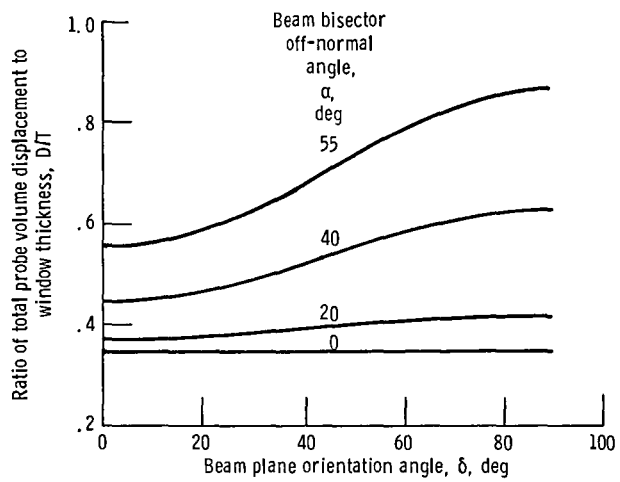
Figure 2. - Relative total probe volume displacement versus beam plane orientation angle for flat-plate windows at various beam bisector off-normal angles. Beam crossing angle, ε, 9°.
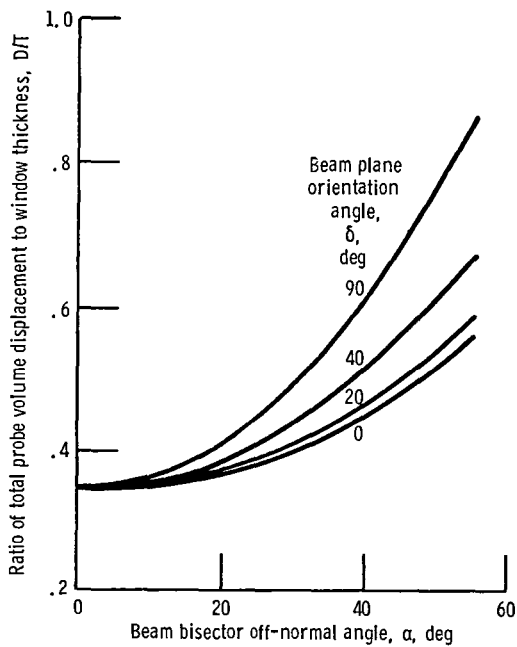
Figure 3. - Relative total probe volume displacement versus beam bisector off-normal angle for flat-plate windows at various beam plane orientation angles. Beam crossing angle, ε, 9°.
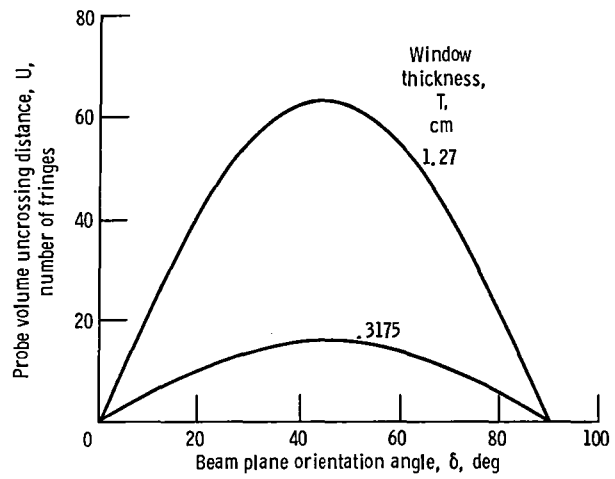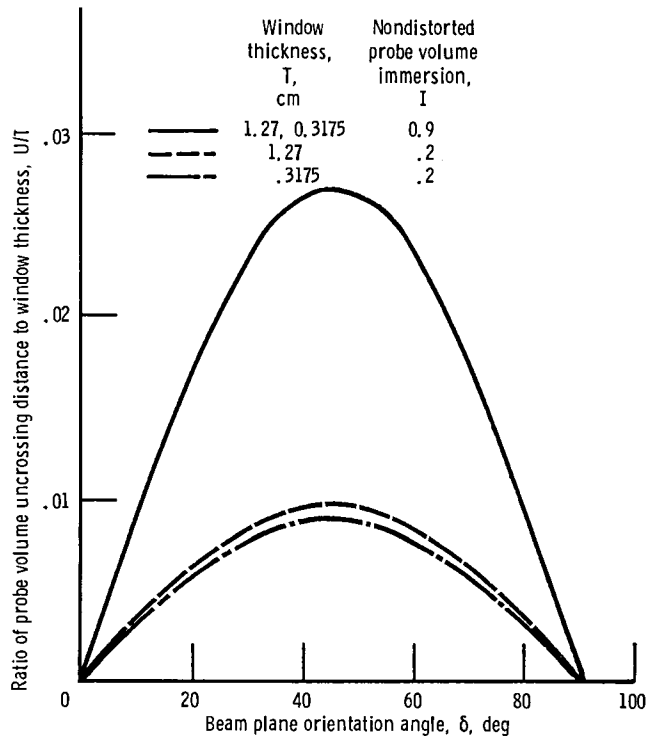
Figure 4. - Probe volume uncrossing distance versus beam plane orientation angle for flat-plate windows at two window thicknesses. Beam bisector off-normal angle, σ, 40°; beam crossing angle, ϵ, 9°.

(a) For beam crossing angles ε of 2.5°, 9°, and 18°.

(b) For all beam crossing angles.
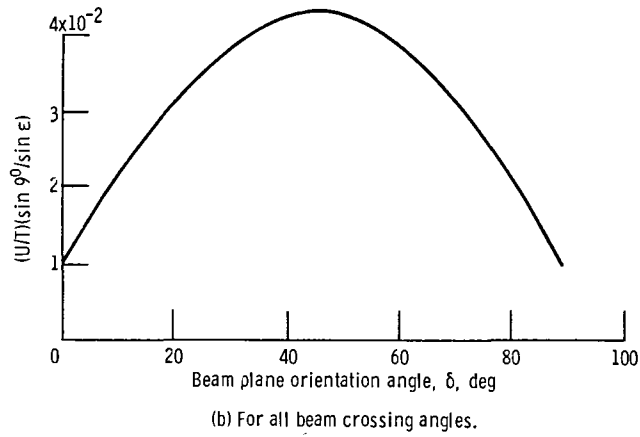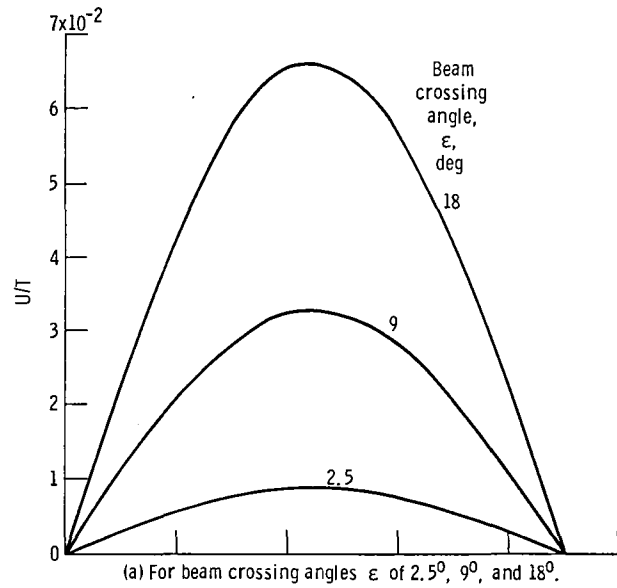
Figure 5. - Relative beam uncrossing distance versus beam plane orientation angle for flat-plate windows. Beam bisector off-normal angle, α, 55°.
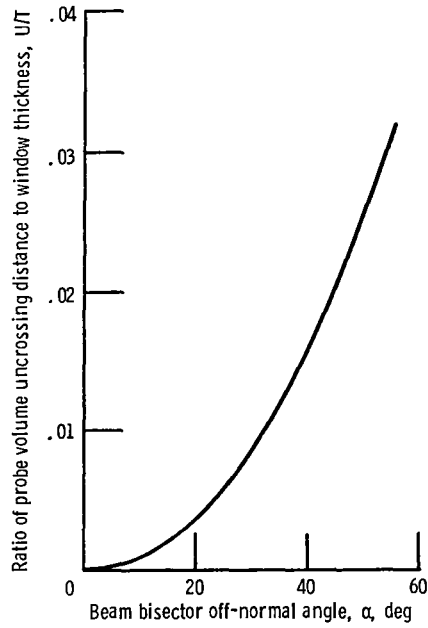
Figure 6. - Relative beam uncrossing distance versus beam bisector off-normal angle for flat-plate windows. Beam plane orientation angle, δ, $40°$.
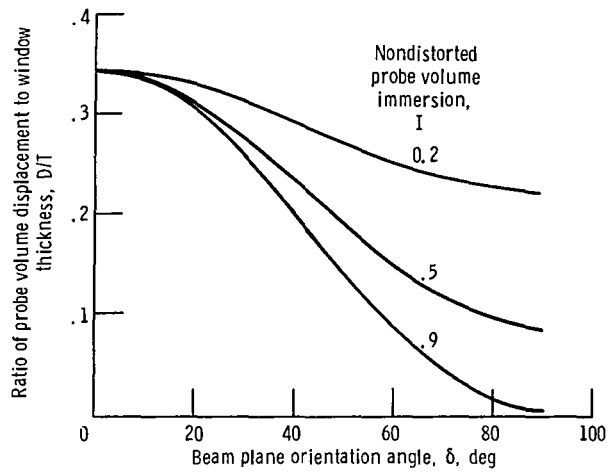
Figure 7. - Relative total probe volume displacement versus beam plane orientation angle for cylindrical windows at various immersions. Window thickness, T, 0.3175 cm; radius of cylindrical window outer surface, R_{CO}, 25.4 cm.
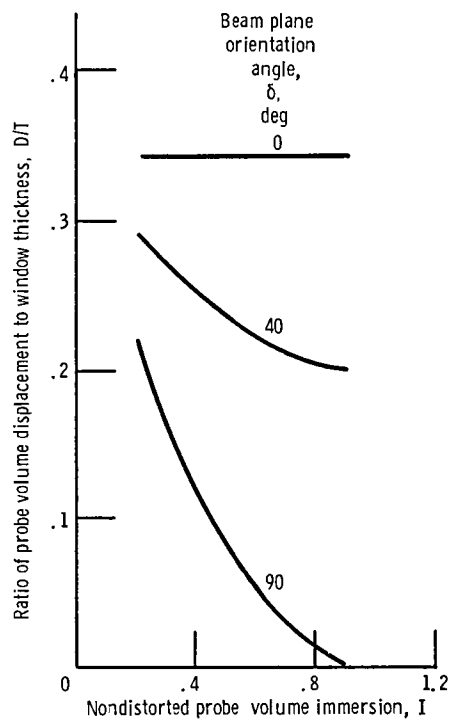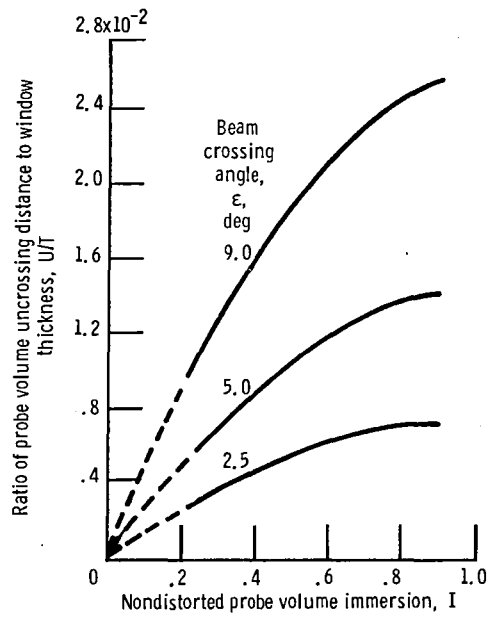
Figure 8. - Relative total probe volume displacement versus nondistorted probe volume immersion for cylindrical windows at various beam plane orientation angles. Beam crossing angle, ϵ, 9^0; window thickness, T, 0.3175 cm; radius of cylindrical window outer surface, R_{CO}, 25.4 cm.
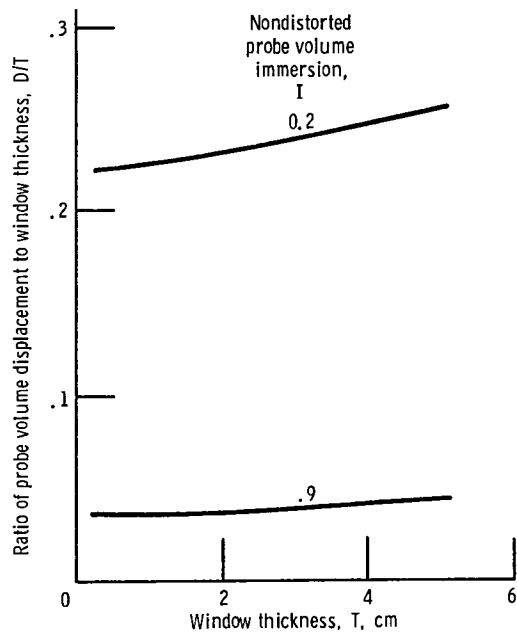
Figure 9. – Relative total probe volume displacement versus window thickness for cylindrical windows at various immersions. Beam plane orientation angle, δ, 90°; radius of cylindrical window outer surface, R_{CO}, 25.4 cm.
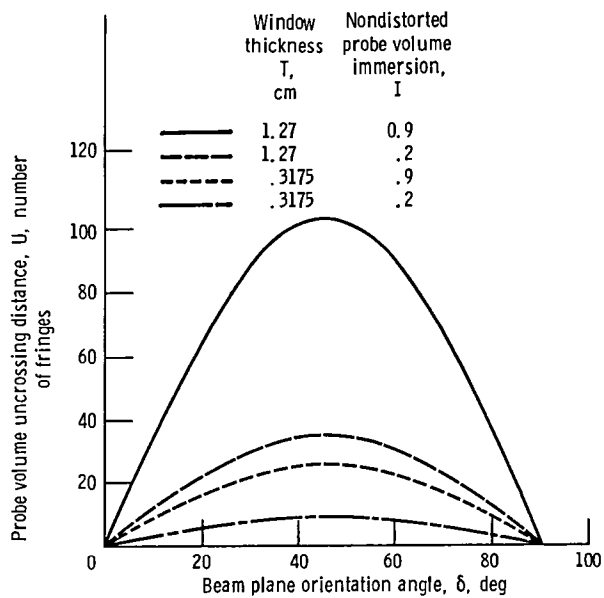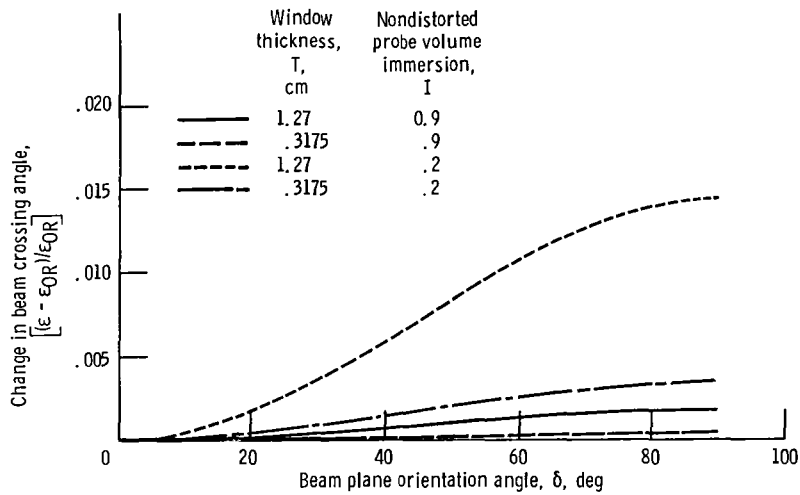

Figure 10. – Probe volume uncrossing distance versus beam plane distortion angle for cylindrical windows at various window thicknesses and immersions. Beam crossing angle, ϵ, 9°; laser light wavelength, λ, 5145 A; radius of cylindrical window outer surface, R_{CO}, 25.4 cm.

Figure 11. - Relative probe volume uncrossing distance versus beam
plane orientation angle for cylindrical windows at various window
thicknesses and immersions. Beam crossing angle, ε, 9°.
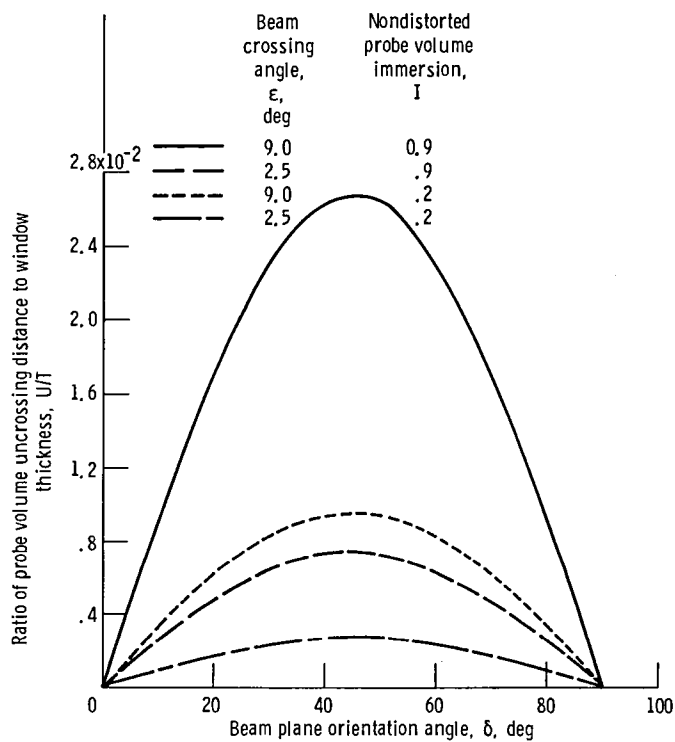
Figure 12. - Relative probe volume uncrossing distance versus beam
plane orientation angle for cylindrical windows at various beam
crossing angles and immersions. Window thickness, T, 0.3175 cm.

Figure 13. - Relative probe volume uncrossing
distance versus immersion for cylindrical
windows at various beam crossing angles.
Beam plane orientation angle, δ, 40°;
window thickness, T, 0.3175 cm.

Figure 14. - Change in beam crossing angle versus beam plane orientation angle
for cylindrical windows at various window thicknesses and immersions. De-
sign beam crossing angle, ϵ, 9°; radius of cylindrical window outer surface;
R_{CO}, 25.4 cm.
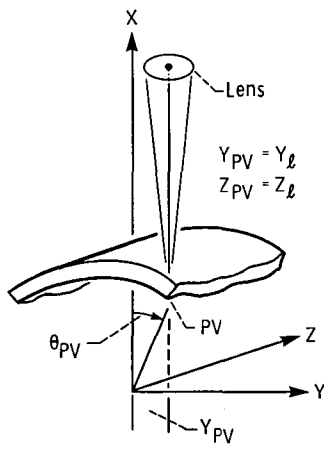
(a) Simple cylinder geometry, non-symmetric case in X-Y (R-θ) plane.
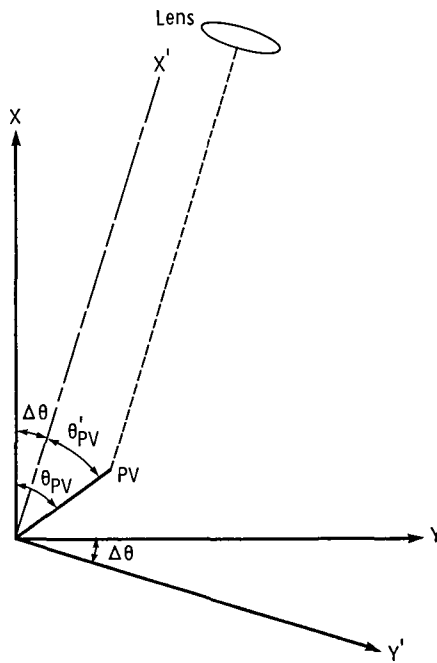
(b) All geometries with beam bisector in R-θ plane.

Figure 15. - Cylinder geometries.
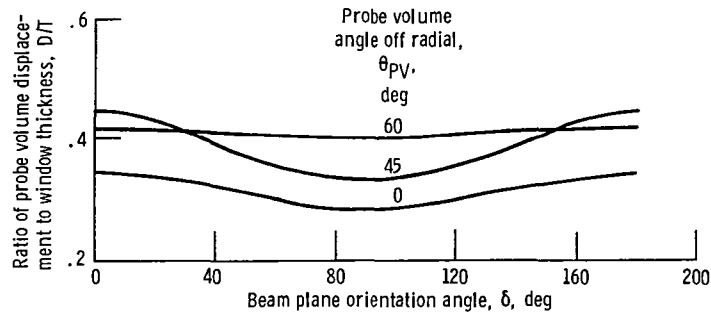
Figure 16. - Relative total probe volume displacement versus beam plane orientation angle for cylindrical windows at various probe volume angles. Beam crossing angle, ε, 9^0; window thickness, T, 1.27 cm; nondistorted probe volume immersion, I, 0.1.
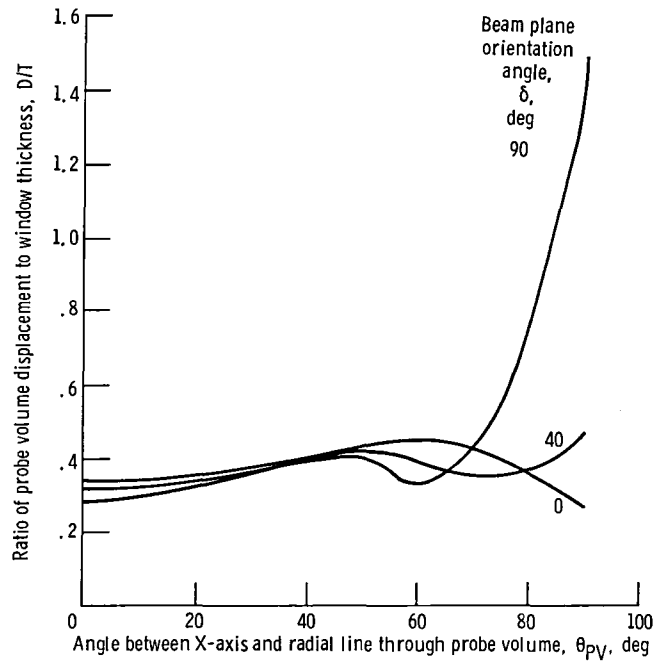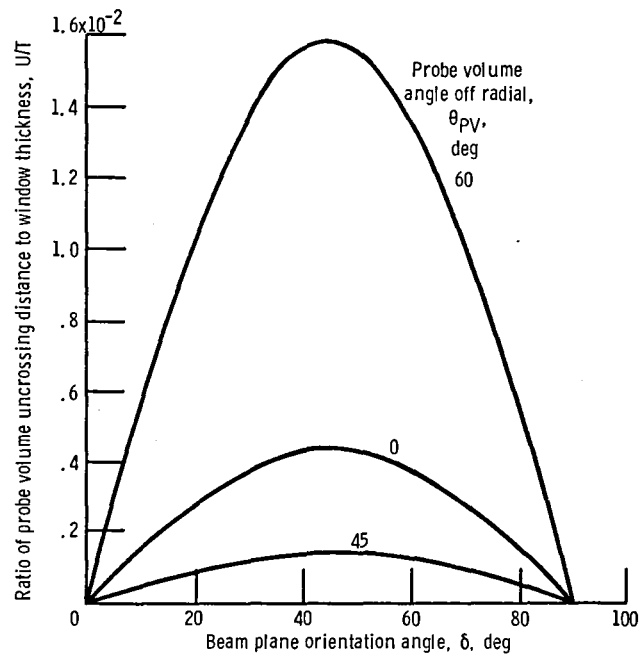

Figure 17. - Relative total probe volume displacement versus probe volume angle off radial for cylindrical windows at various beam plane orientation angles. Beam crossing angle, ε, 9^0; window thickness, T, 1.27 cm; nondistorted probe volume immersion, I, 0.1.

Figure 18. - Relative probe volume uncrossing distance versus beam plane orientation angle for cylindrical windows at various probe volume angles. Beam crossing angle, ϵ, 9^0; window thickness, T = 1.27 cm; nondistorted probe volume immersion, I, 0.1.
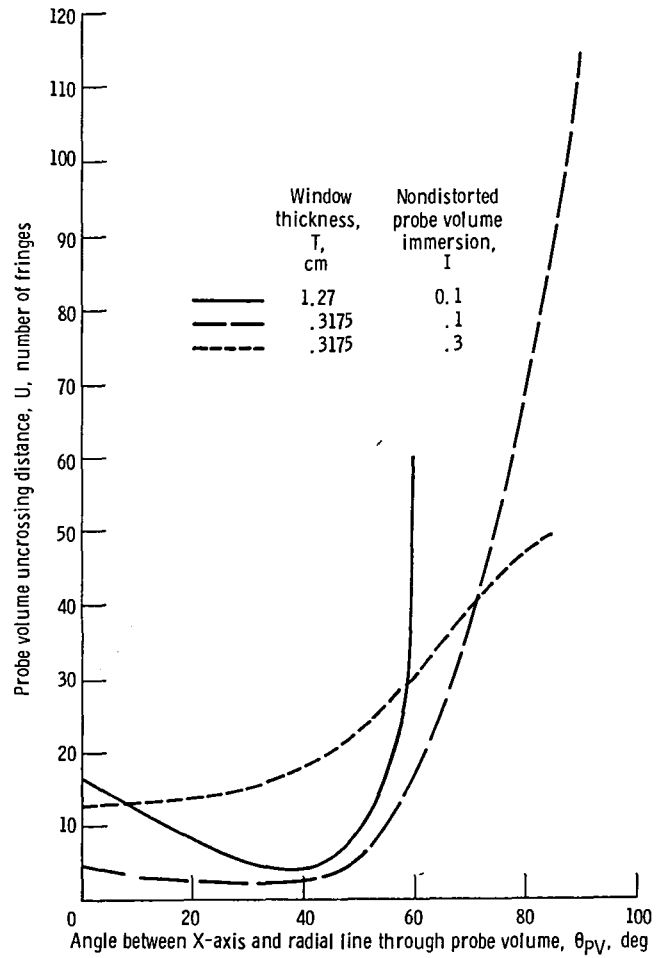
Figure 19. - Probe volume uncrossing distance versus probe volume
angle off radial for cylindrical windows at various window thick-
nesses and immersions. Beam plane orientation angle, δ, 40°;
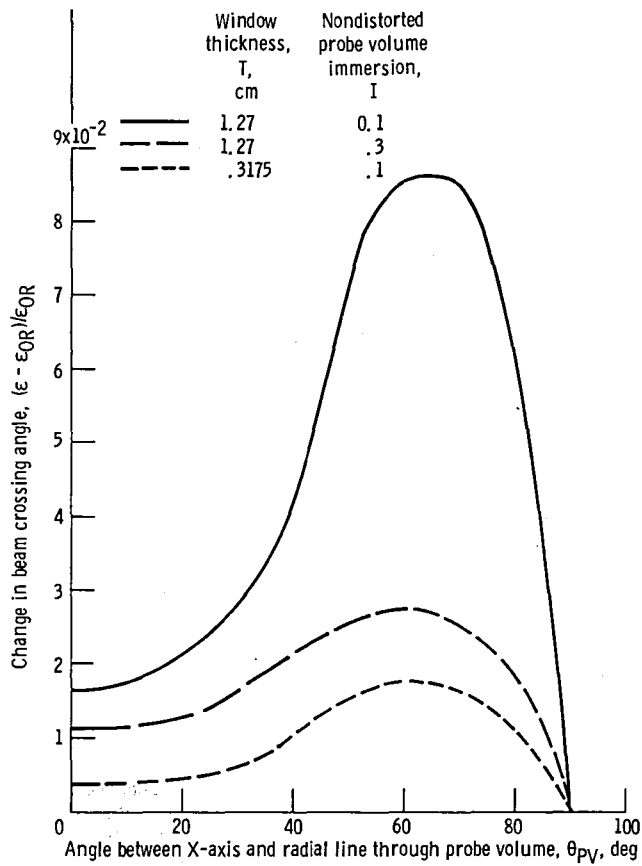beam crossing angle, ε, 9°.

Figure 20. - Change in beam crossing angle versus probe volume angle off radial for cylindrical windows at various window thicknesses and immersions. Beam plane orientation angle, δ, 90°; beam crossing angle, ε, 9°.
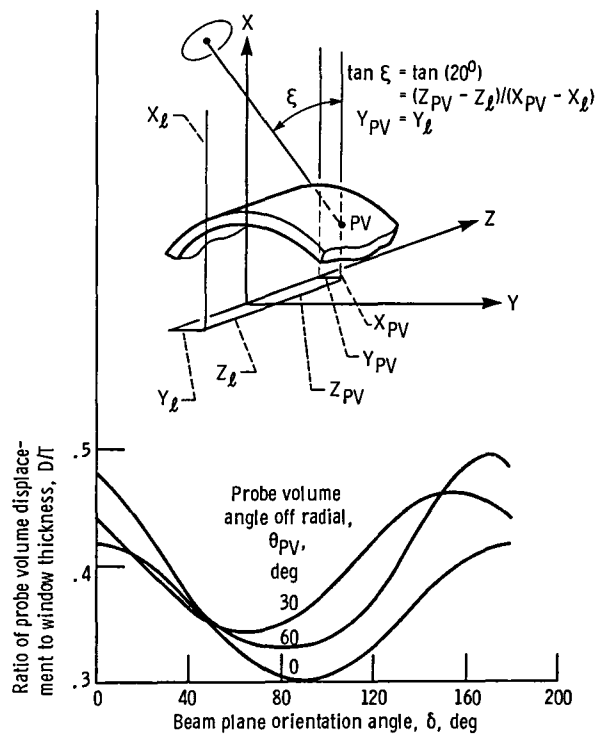
Figure 21. - Relative total probe volume displacement versus beam plane orientation angle for cylindrical windows at various probe volume angles. Beam crossing angle, ε, $9°$; window thickness, T, 0.3175 cm; nondistorted probe volume immersion, I, 0.1; out-of-plane angle of bisecting line relative to x-y plane, ξ, $20°$.
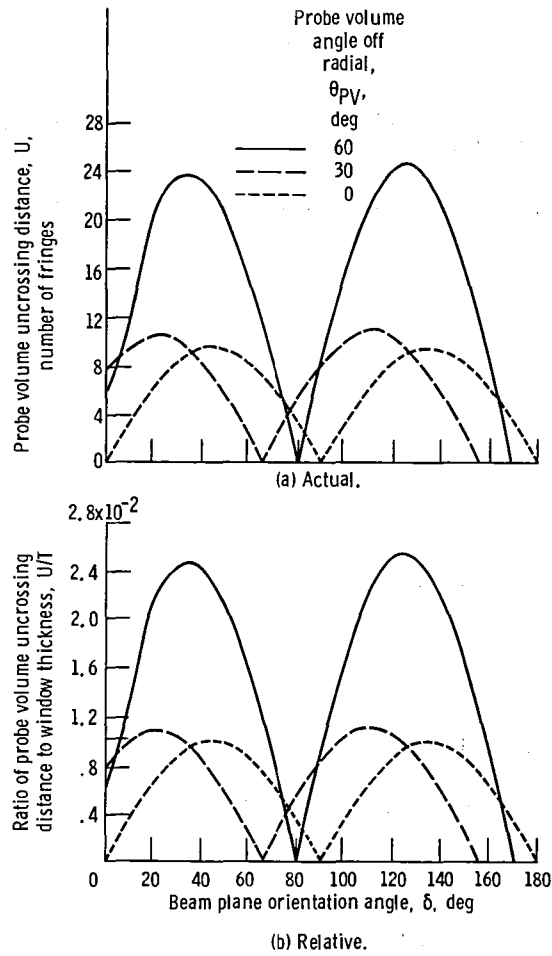
(a) Actual.

(b) Relative.

Figure 22. - Actual and relative probe volume uncross-
ing distances versus beam plane orientation angle for
cylindrical windows at various probe volume angles.
Beam crossing angle, ε, 9^0; laser light wavelength, λ,
5145 A; window thickness, 0.3175 cm; nondistorted
probe volume immersion, I, 0.1; out-of-plane angle
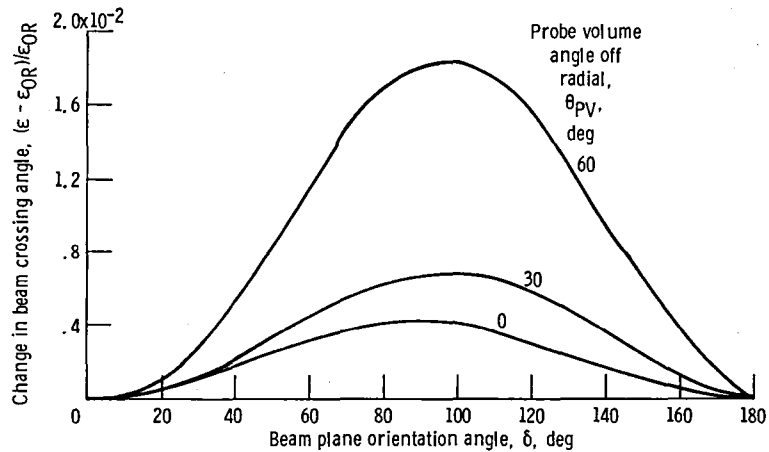of bisecting line relative to x-y plane, ξ, 20^0.

Figure 23. - Change in beam crossing angle versus beam plane orientation angle
for cylindrical windows at various probe volume angles. Beam crossing angle,
ε, 9^0; laser light wavelength, λ, 5145 A; nondistorted probe volume immer-
sion, I, 0.1; out-of-plane angle of bisecting line relative to x-y plane, ξ, 20^0.

1. Report No. NASA TM-87350 USAAVSCOM-TR-86-C-16	2. Government Accession No.	3. Recipient's Catalog No.
4. Title and Subtitle Parametric Study of Beam Refraction Problems Across Laser Anemometer Windows		5. Report Date June 1986
		6. Performing Organization Code 505-62-22
7. Author(s) Albert K. Owen		8. Performing Organization Report No. E-3064
		10. Work Unit No.
9. Performing Organization Name and Address NASA Lewis Research Center and Propulsion Directorate, U.S. Army Aviation Research and Technology Activity - AVSCOM, Cleveland, Ohio 44135		11. Contract or Grant No.
		13. Type of Report and Period Covered Technical Memorandum
12. Sponsoring Agency Name and Address National Aeronautics and Space Administration, Washington, D.C. 20546, and U.S. Army Aviation Systems Command, St. Louis, Mo. 63120		14. Sponsoring Agency Code

15. Supplementary Notes

Part of this material was presented at the Third International Symposium on Applications of Laser Anemometry to Fluid Mechanics, sponsored by the Instituto Superior Tecnico, Lisbon, Portugal, July 7-9, 1986.

16. Abstract

The experimenter is often required to view flows through a window with a different index of refraction than either the medium he is observing or the medium that the laser anemometer is immersed in. The refraction that occurs at the window surfaces may lead to undesirable changes in probe volume position or beam crossing angle and can lead to partial or complete beam uncrossing. This report describes the results of a parametric study of this problem using a ray tracing technique to predict these changes. The windows studied are a flat plate and a simple cylinder. For the flat-plate study (1) surface thickness, (2) beam crossing angle, (3) bisecting line - surface normal angle, and (4) incoming beam plane surface orientation were varied. For the cylindrical window additional parameters were also varied: (1) probe volume immersion, (2) probe volume off-radial position, and (3) probe volume position out of the R-θ plane of the lens. A number of empirical correlations were deduced to aid the interested reader in determining the movement, uncrossing, and change in crossing angle for a particular situation.

17. Key Words (Suggested by Author(s)) Laser anemometry; Refraction; Optical ray tracing	18. Distribution Statement Unclassified - unlimited STAR Category 35
19. Security Classif. (of this report) Unclassified	20. Security Classif. (of this page) Unclassified	21. No. of pages	22. Price*

End of Document